 Bull. Chem. Soc. Jpn., 75, 1977–1982 (2002)

Synthesis of Mono-Dispersed Mesoporous Silica Spheres with Hexagonal Symmetry

Kazuhisa Yano,* Noritomo Suzuki, Yuusuke Akimoto, and Yoshiaki Fukushima

Toyota Central Research & Development Labs. Inc., Nagakute, Aichi 480-1192

(Received November 1, 2001)

Mono-dispersed mesoporous silica spheres with ordered hexagonal regularity were synthesized from tetramethoxysilane and dodecyltrimethylammonium bromide as a surfactant under very specific conditions. By adjusting the optimum concentrations of the reactants, silica particles with diverse morphology were obtained at higher initial concentrations. Dilution of the reactants led to the formation of silica spheres with various sizes and relatively less mesoporous regularity. Mono-dispersed silica spheres could not be obtained when hexadecyltrimethylammonium bromide and tetradecyltrimethylammonium bromide were used as surfactants.

After the discovery of the M41S family,[1] a considerable amount of research has been conducted on the synthesis of mesoporous silica with uniform mesopores and high specific surface areas. Also, the incorporation of various metal species has been attained into the mesoporous structure. Owing to these special characteristics, mesoporous silica can be used exceptionally as catalysts and adsorbents. The morphological control in these materials is one of the main subjects toward their industrial applications. Various reports have revealed that fibers,[2,3,4] sponge-like membranes,[5,6] rod-like powders,[7] films,[8] polyhedral particles[9,10,11] and spheres[12,13,14] have been synthesized. Among these, spherical mesoporous silica is of great interest for applications in chromatography separation and cosmetics.

The synthesis of the first nonporous mono-dispersed silica spheres in the micron size range was developed by Stöber in 1968[15] by employing a water–alcohol–ammonia–tetraalkoxysilane system. Later, in a continuation of this work, mesoporous silica spheres were also synthesized using modified methods. In another report, the synthesis of mono-dispersed silica spheres using long chain alkylamines and tetraethoxysilane[16] (TEOS) was also reported. Although the formed spheres were very fine, the material was poorly ordered with quite lower specific surface areas and pore volumes. Further, ordered mesoporous silica having a high specific surface area was synthesized using hexadecyltrimethylammonium bromide (C_{16}TMABr) or hexadecyltrimethylpyridinium chloride (C_{16}TMPrCl) as a surfactant with a distorted shape.[17] Large mesoporous mono-dispersed spheres with a low specific surface area were obtained[18] when homo-polymers were used as a template. Attempts were also made to prepare mesoporous silica spheres[19] using *N*,*N*-dimethlformamide instead of alcohols as a solvent that also consists of macroporous phases. So far, only a few reports exist concerning the synthesis of mesoporous silica with both a uniform morphology and an ordered mesoporous regularity.

Among the several methods employed for the synthesis of a mesoporous material, a hydrothermal synthesis in a high-pressure bottle is widely adapted, where precise control of the precipitation is rather difficult. In other cases, for example FSM,[20] where material is synthesized by gradual precipitation upon the continuous addition of a dilute HCl solution, the resulting composition of FSM material is far from uniform, because precipitation occurs at different times and pH. In similar synthesis processes, surfactant-templated silica (STS) could be obtained from C_{16}TMABr and tetramethoxysilane (TMOS) in a water-alcohol mixture at ambient temperature.[21,22] During the synthesis, a clear transparent solution gradually becomes turbid, and then precipitation occurs. This has made STS to be a potential method with controlled precipitation toward the formation of uniform mesoporous silica materials.

Here, we describe the modified synthesis of mesoporous silica spheres that consists of both a mono-dispersed spherical morphology and an ordered mesoporous hexagonal regularity. The materials were characterized using X-ray diffraction and transmission electron microscopy. We also investigated the effect of alkyl-trimethylammonium bromide (ATMABr) type and a systematic variation in the concentrations of the reactants for the synthesis of mono-dispersed mesoporous silica spheres.

Experimental

Synthesis. ATMABr (C_{16}TMABr, C_{14}TMABr, C_{12}TMABr; Tokyo Kasei) and TMOS (Tokyo Kasei), a 1 M sodium hydroxide solution and methanol (Wako Inc.) were used without further purification. In the typical synthesis procedure, 0.42 g of C_{12}TMABr and 0.75 mL of 1 M sodium hydroxide solution were dissolved in 100 g of a water/methanol (75/25 = w/w) solution. Then, 0.46 g of TMOS was added to the solution with vigorous stirring at 298 K. After the addition of TMOS, the clear solution gradually turned opaque, resulting in a white precipitate. After 8 h of continuous stirring, the mixture was aged over night. The white powder was then filtered and washed with distilled water at least three times, and dried at 318 K for 72 h. The obtained powder was calcined in air at 823 K for 6 h to remove the organic species. The incorporation of platinum was performed in two separate steps, as

Table 1. Shapes of Particles Obtained from C_{16}TMABr and TMOS

No.	Concentration of C_{16}TMABr/mol dm^{-3}	Concentration of TMOS/mol dm^{-3}	C_{16}TMABr/TMOS*	Precipitation time**/s	Shapes of particle
H1	0.052	0.41	0.13	6	irregular
H2	0.052	0.20	0.26	—***	—****
H3	0.052	0.14	0.37	—***	—****
H4	0.052	0.082	0.63	—***	—****
H5	0.026	0.21	0.12	12	irregular
H6	0.021	0.041	0.51	—***	—****
H7	0.013	0.021	0.62	—***	—****
H8	0.010	0.082	0.12	21	irregular
H9	0.010	0.041	0.24	—***	—****
H10	0.0052	0.041	0.13	47	ellipsoid
H11	0.0026	0.021	0.13	58	sphere
H12	0.0010	0.041	0.25	44	—****
H13	0.0010	0.0082	0.13	140	sphere

*Calculated from concentration of C_{16}TMABr and TMOS.
**Time precipitates appear after the addition of TMOS.
***Precipitation time could not be measured because of subtle change of solution.
****Precipitation could not be recovered from the solution.

described elsewhere.[23]

Characterization. Calcined samples were characterized by transmission electron microscopy and X-ray diffraction measurements. A transmission electron micrograph was obtained with a Jeol-200CX TEM using an acceleration voltage of 200 kV. The average particle size was determined by measuring the size of 50 particles on a TEM picture. A powder X-ray diffraction measurement was carried out with a Rigaku Rint-2200 X-ray diffractometer using Cu-$K\alpha$ radiation. The argon adsorption isotherm was measured using a Quantachrome Autosorb-1 at -87 K. The sample was evacuated at 453 K under 10^{-3} mmHg before the measurement. The pore diameter was calculated using the HK method. A thermogravimetric analysis was performed with a Rigaku Thermo-plus under a nitrogen atmosphere with a heating rate of 10 K min^{-1}.

Results and Discussion

C_{16}TMABr is the mostly used template for the surfactant-assisted synthesis of mesoporous materials. Micelles of an ATMABr tend to be disordered as the length of the alkyl-chain decreases. The disordered mesoporosity of mesoporous materials was very high when C_{10}TMABr or C_8TMABr was used as a template. Because the purpose of presented work was to obtain a uniform mesoporous material, we used C_{16}TMABr, C_{14}TMABr and C_{12}TMABr as surfactants.

The details of the morphologies of the particles obtained using C_{16}TMABr with TMOS at various concentrations are listed in Table 1. In a typical STS synthesis,[21,22] nearly the concentration of H1 was adopted. The precipitates formed quickly (~6 sec) and the shape was irregular. The concentration was varied from this value to a lower one in order to delay the formation of precipitates. Transmission electron micrographs of samples obtained from C_{16}TMABr and TMOS are shown in Fig. 1. Over the range of the surfactants and TMOS concentrations studied, particles of irregular shape and ellipsoid morphology were obtained (Figs. 1a–d; sample H1, H5, H8 and H10 respectively). However, with lower surfactant and silica concentrations (sample H11 and H13) the spherical morphology was observed (Figs. 1e and 1f). In this case, precipitate formation was somewhat delayed ($>$ 58 sec) compared to other samples prepared using C_{16}TMABr. X-ray diffraction patterns of samples with different C_{16}TMABr and TMOS concentrations are shown in Fig. 2. Materials obtained at higher concentrations show low-angle diffraction peaks for the (100), (110) and (200) planes, that confirming the materials were of mesoporous hexagonal regularity. However, the diffraction peaks for the (110) and (200) planes become ambiguous for materials obtained at lower concentrations. In the case of particles with spherical morphology (H13), the diffraction peaks for the (110) and (200) planes could not be distinguished. This fact reveals that the hexagonal regularity of H13 is low. With de-

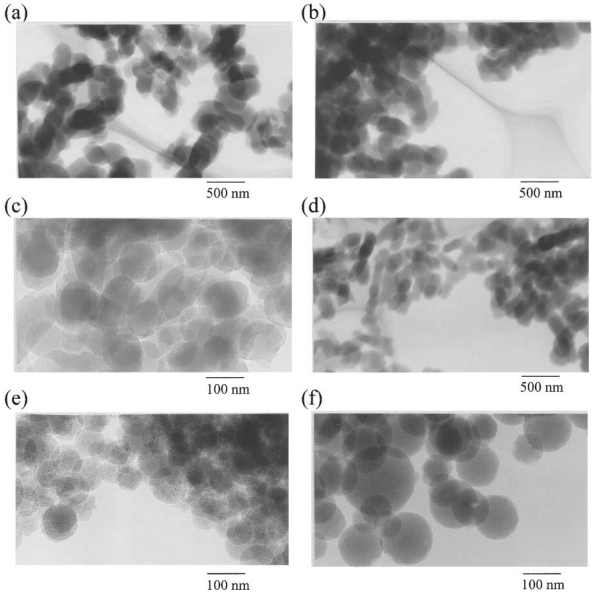

Fig. 1. Transmission electron micrographs of (a) H1, (b) H5, (c) H8, (d) H10, (e) H11, and (f) H13.

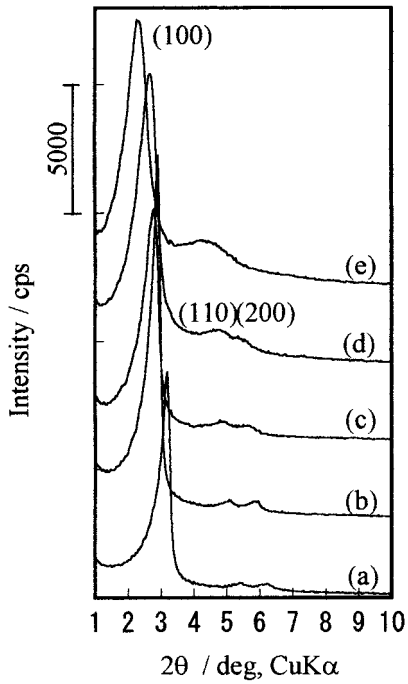

Fig. 2. X-ray diffraction patterns of (a) H1, (b) H5, (c) H8, (d) H10, and (e) H13. The patterns are in the same scale and shifted appropriately.

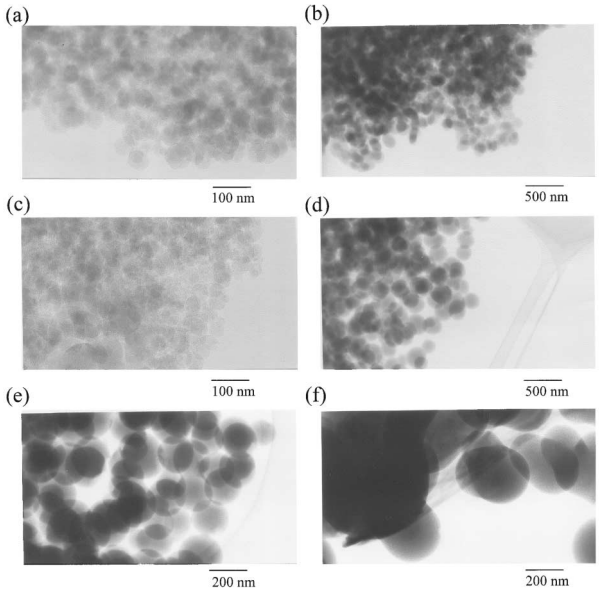

Fig. 3. Transmission electron micrographs of (a) T1, (b) T3, (c) T6, (d) T8, (e) T10, and (f) T12.

creasing concentration of the reactants, the XRD peaks shifted to lower 2-theta values, indicating enlargements of the pore diameters. A TGA measurement revealed that the organic/inorganic molar ratio of every sample was ~0.15 (calculated from the mass reduction of an as-synthesized sample between 423 K and 873 K). When the C_{16}TMABr/TMOS ratio (= organic/inorganic molar ratio) was > 0.15, it was not possible to recover the precipitate from the dark milky color emulsion, even by centrifugation. Agglomeration of the primary particles could be prevented by using an excess amount of C_{16}TMABr, which is also expected to stabilize the primary particles by surrounding the surface.

The results were similar to those of samples obtained form C_{14}TMABr and TMOS. When the C_{14}TMABr/TMOS ratio was > 0.13, the precipitate could not be recovered, except for T9. Details of the morphologies of the particles obtained using C_{14}TMABr with TMOS at various concentrations are listed in Table 2. Transmission electron micrographs of the samples are shown in Fig. 3. The particles are irregular and of ellipsoidal shape at higher concentrations of the reactants (Figs. 3a–c; sample T1, T3, and T6, respectively). However, spherical particles were obtained with lower surfactant and silica concentrations (Figs. 3d–3f; sample T9, T10 and T12). The precipitation time of those samples was somewhat delayed compared to that of other samples. X-ray diffraction patterns of samples

Table 2. Shapes of Particles Obtained from C_{14}TMABr and TMOS

No.	Concentration of C_{14}TMABr/mol dm^{-3}	Concentration of TMOS/mol dm^{-3}	C_{14}TMABr/TMOS*	Precipitation time**/s	Shapes of particle
T1	0.052	0.41	0.13	6	irregular
T2	0.052	0.082	0.63	—***	—****
T3	0.026	0.21	0.12	12	ellipsoid
T4	0.021	0.041	0.51	—***	—****
T5	0.013	0.021	0.62	—***	—****
T6	0.010	0.082	0.12	21	irregular
T7	0.010	0.041	0.24	—***	—****
T8	0.0052	0.041	0.13	46	distorted sphere
T9	0.0052	0.021	0.25	84	sphere
T10	0.0026	0.021	0.13	102	sphere
T11	0.0010	0.041	0.25	40	—****
T12	0.0010	0.0082	0.13	320	sphere & sheet

*Calculated from concentration of C_{14}TMABr and TMOS.
**Time precipitates appear after the addition of TMOS.
***Precipitation time could not be measured because of subtle change of solution.
****Precipitation could not be recovered from the solution.

Table 3. Shapes of Particles Obtained from C_{12}TMABr and TMOS

No.	Concentration of C_{12}TMABr/mol dm^{-3}	Concentration of TMOS/mol dm^{-3}	C_{12}TMABr/TMOS*	Precipitation time**/s	Shapes of particle
D1	0.052	0.41	0.13	6	ellipsoid and sphere
D2	0.052	0.082	0.63	9	ellipsoid
D3	0.026	0.21	0.12	19	sphere, partly adhered
D4	0.024	0.028	0.84	56	monodispersed sphere
D5	0.019	0.028	0.67	58	monodispersed sphere
D6	0.014	0.028	0.50	56	monodispersed sphere
D7	0.0094	0.016	0.59	107	sphere
D8	0.0047	0.012	0.39	158	sphere

*Calculated from concentration of C_{12}TMABr and TMOS.
**Time precipitates appear after the addition of TMOS.

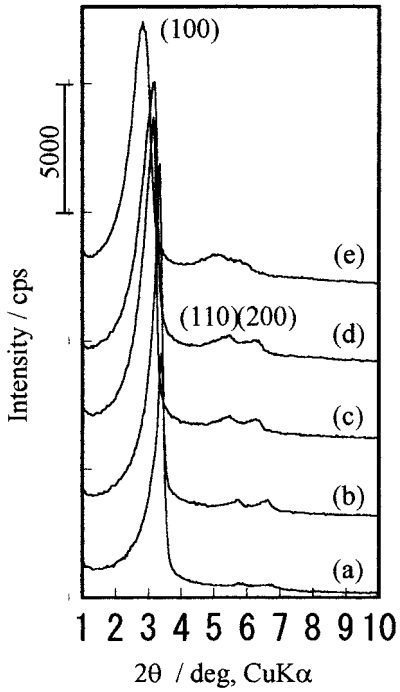

Fig. 4. X-ray diffraction patterns of (a) T1, (b) T3, (c) T6, (d) T8, and (e) T10. Patterns are in the same scale and shifted appropriately.

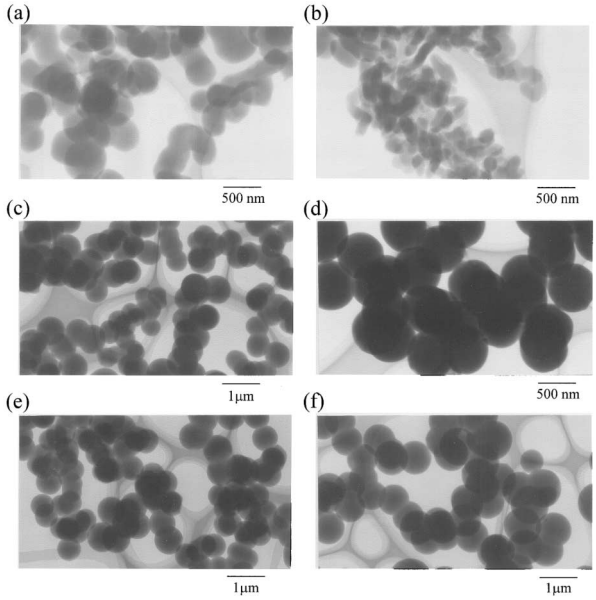

Fig. 5. Transmission electron micrographs of (a) D1, (b) D2, (c) D3, (d) D6, (e) D7, and (f) D8.

with different C_{14}TMABr and TMOS concentrations are shown in Fig. 4. There are three peaks assigned to the diffraction of the (100), (110) and (200) planes due to the hexagonal regularity. These peaks are shifted to lower 2-theta values, and the diffraction peaks for (110) and (200) planes becomes ambiguous with decreasing concentration of the reactants, further indicating an enlargement of the pore diameters and disordering of the hexagonal regularity.

The results with C_{12}TMABr were amazingly different from those with C_{16}TMABr or C_{14}TMABr surfactants. Details of the morphologies of the particles obtained using C_{12}TMABr with TMOS at various concentrations are listed in Table 3. Transmission electron micrographs of these samples are shown in Fig. 5. Although particles are ellipsoidal at higher concentrations of the reactants (sample D1 and D2), most of the particles obtained were spherical over a wide range of experimental concentrations. In the case of C_{12}TMABr, perhaps the agglomeration of the primary particles was not prevented by an excess amount of the surfactant. In particular, mono-dispersed spheres were obtained when the concentrations of TMOS and C_{12}TMABr were 0.028 M and 0.014–0.024 M, respectively (sample D4–D6). These concentrations are very low (∼1/10) compared to the commonly used synthetic conditions.[1,20] The average diameter of the particles was 640 nm in the case of D6. Moreover, spheres with various sizes could be obtained at lower concentrations of the reactants (sample D7 and D8). The X-ray diffraction patterns of these samples are given in Fig. 6 and confirm the highly ordered hexagonal regularity (sample D6). Similar patterns were obtained for D1–D5 samples (XRD patterns not shown). With decreasing concentration of the surfactant and silica, the peak of the (100) plane diffraction shifted to a lower 2-theta value (sample D7 and D8), and the peaks of the (100) and (210) planes became ambiguous. This fact indicates an enlargement of the mesopores and a disordering of the hexagonal regularity. The argon adsorption isotherm of sample D6 is shown in Fig. 7. The pore diameter calculated from the

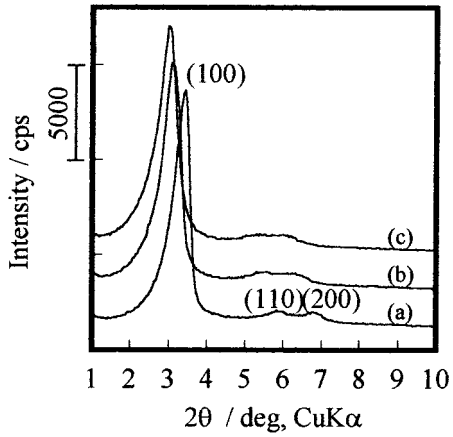

Fig. 6. X-ray diffraction patterns of (a) D6, (b) D7, and (c) D8. X-ray diffraction patterns of D1, D2, and D3 were almost identical to that of D6.

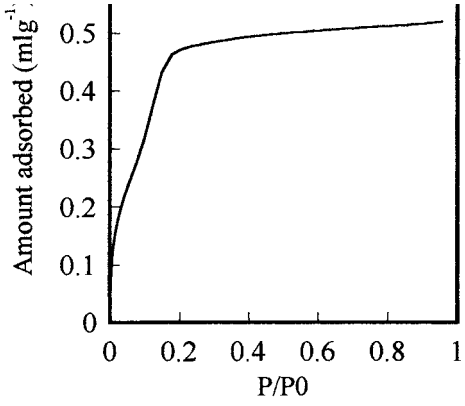

Fig. 7. Argon adsorption isotherm of D6.

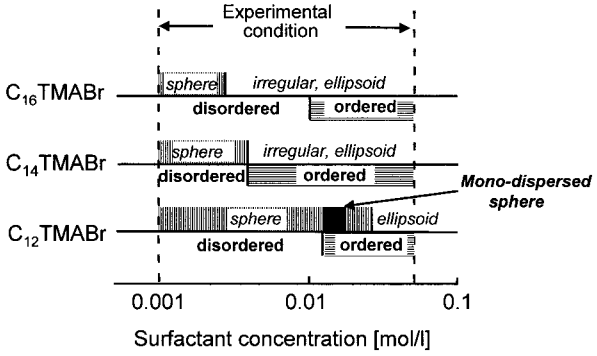

Fig. 8. Effect of surfactant concentration on the morphology and mesoporous regularity of the particle obtained using cationic surfactant with different alkyl-chain length. Morphology (italic); mesoporous regularity (bold).

isotherm is 21.1 Å.

Fig. 8 shows the influence of the surfactant concentration on the morphologies as well as the hexagonal regularity of the materials. Although spherical particles were obtained at lower concentrations when C_{14}TMABr or C_{16}TMABr were used as a surfactant, a mono-dispersed spherical morphology was not observed. However, spherical particles were obtained over a wide range of experimental concentrations with C_{12}TMABr, and a mono-dispersed spherical morphology was observed under specific concentrations. On the other hand, hexagonally ordered mesoporous materials were obtained at higher concentrations regardless of the type of surfactant. Spherical particles with an ordered hexagonal regularity were not obtained when C_{16}TMABr or C_{14}TMABr was used as a surfactant. Only when using C_{12}TMABr were hexagonally ordered spherical particles obtained, and was the synthesis of mono-dispersed mesoporous silica spheres with ordered hexagonal symmetry attained.

From earlier work, it is evident that non-porous spherical silica particles could be formed using alkoxysilanes under basic conditions in the absence of a surfactant.[15] Although no details are available regarding the rate of condensation, it is assumed that the condensation reaction proceeds slowly, since silicic acid esters of a higher alcohol (pentanol) was used as a silica precursor, and the reaction was conducted in an alcoholic solution. Therefore, it is presumed that the formation of spherical particles could be achieved when the condensation reaction proceeds slowly. In this experiment, the precipitation time was longer at lower concentrations compared to higher concentrations (Table 1–3). This result explains the reason why spherical particles were obtained at lower concentrations with any type of surfactant. In addition, the alkyl-chain length of the surfactant also affects the precipitation time. The precipitation time of particles obtained with C_{12}TMABr was longer than that with C_{16}TMABr or C_{14}TMABr (compare H5 in Table 1, T3 in Table 2 and D3 in Table 3). Then, spherical particles were obtained over a wide range of concentrations with C_{12}TMABr. In general, a precipitate appears when particles become large enough to be excluded from a solution by the progress of the condensation reaction. Also, the hydrophobicity of particles plays an important role for precipitation from a water-alcohol system. Because the rate of the condensation reaction should be independent on the type of surfactant, a less hydrophobic property of C_{12}TMABr leads to a longer precipitation time, resulting in an easy formation of spherical particles. However, a more significant aspect of mono-dispersed particle formation is the simultaneous generation, followed by propagation and subsequent termination of each and every particle under a similar rate of condensation. It is worth mentioning here that the later conditions were successively achieved only in the case of C_{12}TMABr.

Further, to address the reaction for the formation of hexagonal symmetry inside a sphere, it is necessary to understand the possible geometries. In general, it is rather difficult to arrange hexagonal columns into a sphere. Therefore, how the hexagonal columns are arranged inside a sphere is of great interest. We followed a very simple strategy, where the internal sphere of D6 was apparently visualized by the partial incorporation of platinum. The TEM of platinum incorporated D6 is shown in Fig. 9. The dark section of the micrograph represents the platinum incorporated into the mesopores. The amount of platinum incorporated was further controlled for better and clearer observation of inside the sphere. Interestingly, arrays of parallel dark lines were observed throughout the sphere. Moreover,

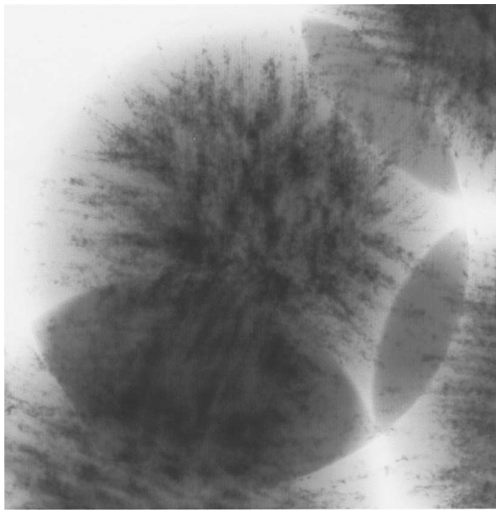

Fig. 9. Transmission electron micrograph of platinum incorporated D6. Dark section represents the platinum.

these arrays were aligned toward the center of the sphere from various possible directions. It is worth mentioning that the mesopores do not form from the center to outside of the sphere radially, and vise-versa. The TEM result describes that the initially formed mesoporous hexagonal arrays simultaneously transformed into particles with spherical morphology.

Conclusions

In summary, mono-dispersed mesoporous silica spheres with highly ordered hexagonal regularity were obtained using C_{12}TMABr as a surfactant. Spherical particles were obtained at lower concentrations while hexagonally ordered mesoporous materials were obtained at higher concentrations with C_{16}TMABr or C_{14}TMABr. However, when using a short-chain surfactant of C_{12}TMABr, spherical particles were obtained over a wide range of experimental concentrations, resulting in the formation of spherical particles with ordered hexagonal regularity. Work is underway to explore new potential applications of these materials.

References

1 C. T. Kresge, M. E. Leonowicz, W. J. Roth, J. C. Vartuli, and J. S. Beck, *Nature*, **359**, 710 (1992); J. S. Beck, J. C. Vartuli, W. J. Roth, M. E. Leonowicz, C. T. Kresge, K. D. Schmitt, C. T. W. Chu, D. H. Olson, E. W. Sheppard, S. B. McCullen, J. B. Higgins, and J. L. Schlenker, *J. Am. Chem. Soc.*, **114**, 10834 (1992).

2 P. Yang, D. Zhao, B. F. Chmelka, and G. D. Stucky, *Chem. Mater.*, **10**, 2033 (1998).

3 P. J. Bruinsma, A.Y. Kim, J. Liu, and S. Baskaran, *Chem. Mater.*, **9**, 2507 (1997).

4 H-P. Lin, L-Y. Yang, C-Y. Mou, H-K. Lee, and S-B. Liu, *Stud. Surf. Sci. Catal.*, **129**, 7 (2000).

5 D. Zhao, P. Yang, B. F. Chmelka, and G. D. Stucky, *Chem. Mater.*, **11**, 1174 (1999).

6 D. Zhao, J. Sun, Q. Li, and G. D. Stucky, *Chem. Mater.*, **12**, 275 (2000).

7 S. Shio, A. Kimura, M. Yamaguchi, K. Yoshida, and K. Kuroda, *Chem. Commun.*, **1998**, 2461.

8 S. H. Tolbert, T. E. Schaffer, J. Feng, P. K. Hansma, and G. D. Stucky, *Chem. Mater.*, **9**, 1962 (1997).

9 J. M. Kim, S. K. Kim, and R. Ryoo, *Chem. Commun.*, **1998**, 259.

10 S. Guan, S. Inagaki, T. Ohsuna, and O. Terasaki, *J. Am. Chem. Soc.*, **122**, 5660 (2000).

11 C. Shunai, Y. Sakamoto, O. Terasaki, and T. Tatsumi, *Chem. Mater.*, **13**, 2237 (2001).

12 L. Qi , J. Ma, H. Cheng, and Z. Zhao, *Chem. Mater.*, **10**, 1623 (1998).

13 H-P. Lin, Y-Ru. Cheng, and C-Y. Mou, *Chem. Mater.*, **10**, 3772 (1998).

14 Q. Huo, J. Feng, F. Schuth, and G. D. Stucky, *Chem. Mater.*, **9**, 14 (1997).

15 W. Stöber and A. J. Fink, *Colloid Interface Sci.*, **26**, 62 (1968).

16 M. Grün, G. Büchel, D. Kumar, K. Schumacher, B. Bidlingmajer, and K. K. Unger, *Stud. Surf. Sci. Catal.*, **128**, 155 (2000).

17 M. Grün, I. Lauer, and K. K. Unger, *Adv. Mater.*, **9**, 254 (1997).

18 K. Schumacher, S. Renker, K. K. Unger, R Ulrich, A. D. Chesne, H. W. Spiess, and U. Wiesner, *Stud. Surf. Sci. Catal.*, **129**, 1 (2000).

19 Q. Luo, L. Li, Z. Xue, and D. Zhao, *Stud. Surf. Sci. Catal.*, **129**, 37 (2000).

20 S. Inagaki, A. Koiwai, N. Suzuki, Y. Fukushima, K. Kuroda, *Bull. Chem. Soc. Jpn.*, **69**, 1449 (1996).

21 M. T. Anderson, J. E. Martin, J. G. Odinek, and P. P. Newcomer, *Chem. Mater.*, **10**, 311 (1998).

22 M. T. Anderson, J. E. Martin, J. G. Odinek, and P. P. Newcomer, *Chem. Mater.*, **10**, 1490 (1998).

23 C. H. Ko and R. Ryoo, *Chem. Commun.*, **1996**, 2467.